Article

Towards Intraoperative Detection of Disseminated Tumor Cells in Lymph Nodes with Silicon Nanowire Field Effect Transistors

Duy P. Tran, Marnie A. Winter, Bernhard Wolfrum, Regina Stockmann, Chih-Tsung Yang, Mohammad P. Moghaddam, Andreas Offenhäusser, and Benjamin Thierry

ACS Nano, **Just Accepted Manuscript** • DOI: 10.1021/acsnano.5b07136 • Publication Date (Web): 09 Feb 2016

Title page

Towards Intraoperative Detection of Disseminated Tumor Cells in Lymph Nodes with Silicon Nanowire Field Effect Transistors

Duy P. Tran[1], Marnie A. Winter[1], Bernhard Wolfrum[2], Regina Stockmann[2], Chih-Tsung Yang[1], Mohammad Pourhassan-Moghaddam[3], Andreas Offenhäusser [2] and Benjamin Thierry[1*]*

[1] Future Industries Institute, University of South Australia, Mawson Lakes Campus, Mawson Lakes, South Australia 5095, Australia

[2] Peter Grünberg Institute, Forschungszentrum Jülich GmbH, Jülich, Germany.

[3] Department of Medical Biotechnology, Tabriz University of Medical Sciences, Tabriz, Iran.

Contact information:

Benjamin Thierry. Phone: +61 8 8302-3689. Fax: +61 8 8302-3683. Email: benjamin.thierry@unisa.edu.au

Andreas Offenhäusser. Phone: +49 246161-2330. Fax: +49 246161-8733. Email: a.offenhaeusser@fz-juelich.de

Towards Intraoperative Detection of Disseminated Tumor Cells in Lymph Nodes with Silicon Nanowire Field Effect Transistors

Duy P. Tran[1], Marnie A. Winter[1], Bernhard Wolfrum[2], Regina Stockmann[2], Chih-Tsung Yang[1], Mohammad P. Moghaddam[3], Andreas Offenhäusser [2] and Benjamin Thierry[1*]*

[1] Future Industries Institute, University of South Australia, Mawson Lakes Campus, Mawson Lakes, South Australia 5095, Australia

[2] Peter Grünberg Institute, Forschungszentrum Jülich GmbH, Jülich, Germany.

[3] Department of Medical Biotechnology, Tabriz University of Medical Sciences, Tabriz, Iran.

KEYWORDS: Intraoperative detection; CMOS; silicon nanowire on a chip; lymph node metastasis, nano fabrication; integrated biosensor; multi-channel detection; diagnostic.

ABSTRACT. Within an hour, as little as one disseminated tumor cell (DTC) per lymph node can be quantitatively detected using an intraoperative biosensing platform based on silicon nanowire field-effect transistors (SiNW FET). It is also demonstrated that the integrated biosensing platform is able to detect the presence of circulating tumor cells (CTCs) in the blood of colorectal cancer patients. The presence of DTCs in lymph nodes and CTCs in peripheral blood are highly significant as it is strongly associated with poor patient prognosis. The SiNW FET sensing platform out-performed in both sensitivity and rapidity not only the current standard method based on pathological examination of tissue sections but also the emerging clinical gold standard based on molecular assays. The possibility to achieve accurate and highly-sensitive analysis of the presence of DTCs in the lymphatics within the surgery timeframe has the potential to spare cancer patients from an unnecessary secondary surgery, leading to reduced patient morbidity, improving their psychological wellbeing and reducing time spent in hospital. This study demonstrates the potential of nanoscale field-effect technology in clinical cancer diagnostics.

Rapid and sensitive molecular analysis of resected human tissues has the potential to drastically improve on current cancer patient's care. An accurate intraoperative molecular diagnosis of cancer metastasis could indeed limit the need for extensive surgery by providing critical information for classifying tumor spread, establish patients' prognosis and appropriate treatment without delay potentially leading to decreased time spent in hospital,[1,2] reduced side effects[3,4] and an improved patient wellbeing.[5] The detection of disseminated tumor cells (DTC) in cancer patient lymph nodes (LNs) is the most important prognostic indicator in a number of different types of cancer.[6,7] In current clinical practice, cytological or immuno-histochemical examination of resected or biopsied lymph nodes is usually performed to determine the presence of disseminated tumor cells. In general, these methodologies are time-consuming, semi-quantitative and have a low reliability to detect cancer cells when dealing with minute amounts of biological samples,[8,9] which is often the case in fine needle biopsied tissues[10] and micrometastases with diameters less than 2 mm. Quantitative real-time polymerase chain reaction (qRT-PCR)[11–13] and tissue microarrays[14,15] have been developed for intraoperative genetic analysis of lymph node metastasis. However, these techniques can be problematic and are often associated with amplification error, label dependence and inaccuracy due to cross-hybridization, and nonspecific absorption. Recently, the one-step-nucleic acid amplification (OSNA) system is rapidly becoming the standard intraoperative method for the detection of DTCs in resected lymph nodes. The OSNA system detects the presence of Cytokeratin 19 mRNA and can confirm the presence of cancer cells within 1 hour after specimen collection.[16,17] The main limitations of the OSNA method include the need for amplification of target RNA, false negative signal from the presence of inhibitors and requirement of a known sequenced target.

Silicon nanowire field-effect transistors (SiNW FETs) provide a promising platform for intraoperative biosensor development, owing to their inherent characteristics, which include fast measurement response (in the order of minutes),[18,19] ultra-high sensitivity (~fM in detection sensitivity) and wide dynamic range,[19,20] label-free detection nature, and compatibility with multiplexed target detection.[21,22] In comparison to PCR or other solid state biosensing technologies such as Surface Plasmon Resonance (SPR) platforms, biosensor-based SiNW FET platforms are in general compact, easy to calibrate, fully compatible with on-chip microfluidic integration as well as handheld device development. Herein, we demonstrate a new concept of an intraoperative biosensor based on SiNW FETs for ultrasensitive, label-free and rapid molecular detection of tumor cells in lymph nodes (LNs). We also demonstrate the versatility and sensitivity of this platform for the direct detection of circulating tumor cells (CTCs) in colorectal cancer patient's peripheral blood. The developed intraoperative biosensor displays a high detection sensitivity for keratin (KRT) (~ 83 fM in 10% serum), used here as a marker for detection of DTC. In a model mimicking micro-metastasis in lymph nodes, the SiNW FET biosensor enabled detection of KRT antigens at a limit of detection (LOD) as low as ~1.3 cancer cells/μL in un-purified LN lysates and within an intraoperative timeframe (*i.e.* 30 minutes). This study demonstrates the feasibility of this SiNW FET sensing platform to achieve rapid and sensitive detection of DTC in biological specimens and therefore it presents itself as a potential alternative to current molecular assays based on the quantification of tumor-specific mRNA markers.[11–13]

RESULTS AND DISCUSSION. The SiNW FETs were fabricated at the wafer-scale and then on-chip packaged in a CMOS-compatible process, which was modified from our published protocol based on electron-beam lithography and tetramethylammonium hydroxide (TMAH) wet-etching.[23,24] In this work, the SiNW FET sensing platform has been re-designed for achieving an optimal compromise between sensitivity and reliability. Details of the electrical characterization of the fabricated devices are reported in the Supporting Information, Note 1. As shown in Figure 1a, a completed test chip SiNW FET (18 × 8 mm) consists of 2 built-in Ag/AgCl reference electrodes, 3 independent sensing channels functionalized with the molecular probe (*e.g.* antibodies), and 1 control channel. Each of the channels consists of 8 identical nanowires with thicknesses of 40 nm, widths of 150 nm, 2 μm wire-to-wire distances and 10 μm lengths. The nanowires are connected to the same Al/Cr/Ag contact line on each side. A low-temperature dry oxidized SiO_2 (10-15 nm) layer has been formed on the nanowires served as a gate dielectric. A thin (~1 μm) passivation layer of SiO_2/Si_3N_4 has been deposited and patterned, aiming for electrically protecting the device's metal contact lines during the wet-measurement. The SiNW chips are packaged in a dual in-line package (DIP-24) ceramic sockets for improving durability and measurement convenience. Electrical measurement of the integrated SiNW FET is performed using a custom-built 16 channel amplifier system (20×10 cm)[25] integrated with a compact head-stage for simultaneous measurement of up to 8 channels (Figure 1b). All measurements were carried out using micro Ag/AgCl reference electrode as liquid front gate.

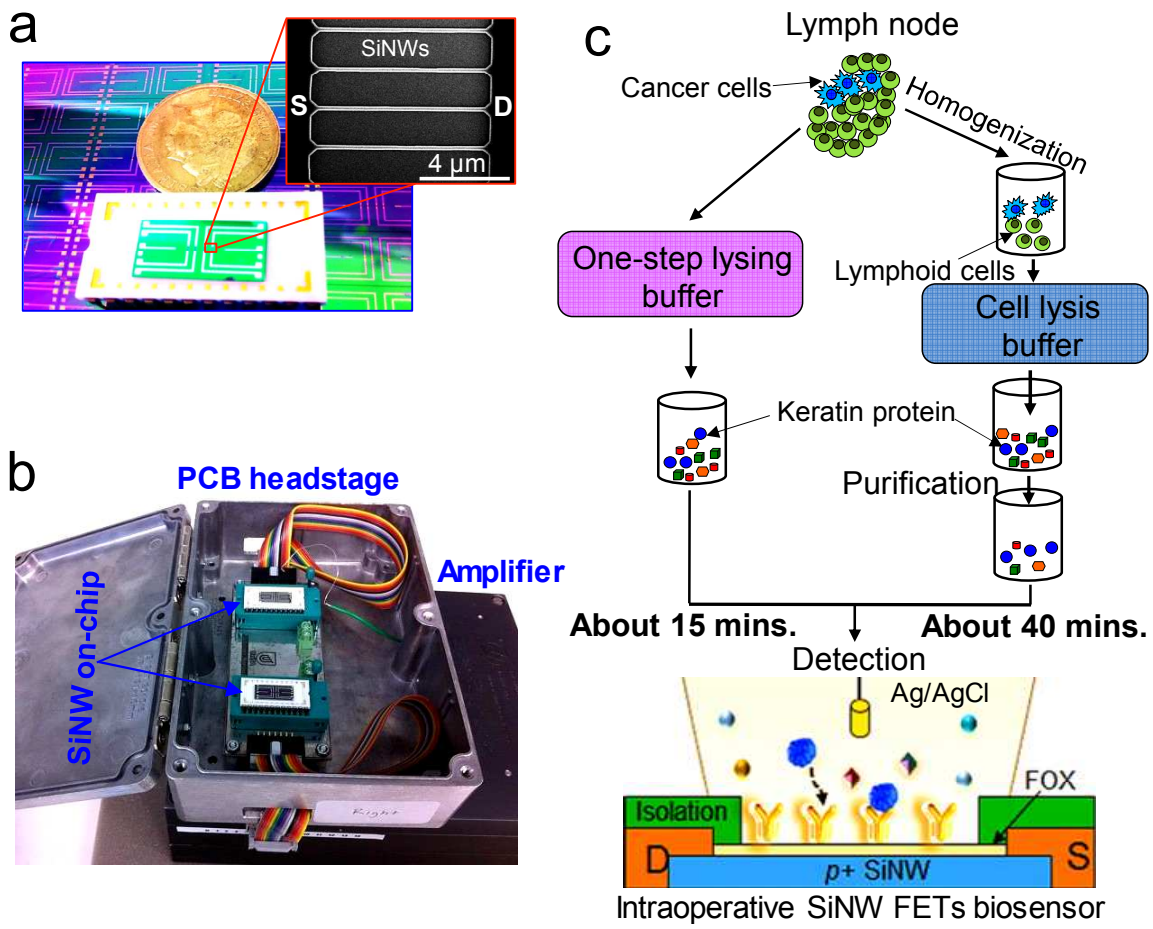

Figure 1. (a) Photographic and SEM images (insert) of a typical SiNW FET array connected to source-drain (S-D) electrodes. (b) Photograph of the 16 channels measurement amplifier with built-in printed circuit board (PCB) head-stage for parallel measurement. (c) Illustration of the measurement procedures of the SiNW FET biosensor. Two different sample preparation schemes were developed (Supporting Note 3). One-step protocol (~15 minutes): LNs spiked with a known number of tumor cells and then directly lysed inside an ultrasonic bath with our developed lysing buffer. Two-step protocol (~40 minutes): LNs spiked with a known number of tumor cells were first homogenized in a standard cell lysing buffer without adding urea additive. The resulting lysate was centrifuged to enrich the insoluble KRT fragments which were later solubilized in the

second step of the method. All measurements were performed in 0.01X PBS (pH 7.4, RT) after thorough washing in 1X PBS.

At first, we investigated the performance of FET biosensors for detection of Cytokeratin-19 (KRT-19) protein spiked in 10% serum. This human recombinant KRT-19 is a single, non-glycosylated polypeptide chain having a molecular mass of 44,098 Dalton and is broadly used for immuno-detection of LN metastases in cancer patients[26–28] as well as for detection of CTCs in patients' blood.[27,29] In this work, the KRT-19 detection was employed to optimize and calibrate the fabricated biosensing devices. A specific challenge associated to bio-FET molecular sensors is the detection of targets (*e.g.* protein or genomic markers) in physiological samples due to their inherent high ionic strengths and the resulting very short Debye lengths (typically λD ~0.7 nm[30,31]). At such short Debye length, charges from the targets are screened and therefore, not readily detected.[30,32] A number of strategies have been proposed to circumvent this issue and enable measurements in biological samples. For instance, an advanced microfluidic pre-isolation/purification concept has been demonstrated.[33] However, in most practical applications, steady-state measurements carried out after a washing step provide suitable controlled measurement conditions. Considering the scope and requirements of the proposed sensing platform, namely intraoperative detection of tumour markers associated to lymphatic involvement, the later measurement strategy was selected to ensure simple and rapid measurements. Prior to measurements, the SiNW FETs were washed with 1X PBS and subsequently with 0.01X PBS, which extended the measurement Debye length to ~ 8 nm. In agreement with previous reports, this provided sufficient sensitivity to detect proteinaceous targets such as KRT.

Figure 2a displays the response of SiNW FETs measured with various KRT-19 concentrations at a constant V_{DS} = -1.5 V. From the graph, it is shown that the transfer characteristic curves shift to more positive gate values (increase of the device's conductance $G=I_{DS}/V_{DS}$) with increasing KRT-19 concentrations from pure serum to 25 nM (~1 μg/mL). In the measured buffer (0.01× PBS, pH 7.4), the increases of nanowire conductivity is extrapolated by the coupling of negatively charged KRT protein (isoelectric point ~5.1[34]) to the anti-KRT antibodies on the SiNW surfaces. The detection sensitivity of SiNW FET biosensors to the KRT targets is dependent on the structure and quality of the devices as well as the Debye length as noted above. It is also directly dependant on the distance of the binding site (*d*BS) of the antigen-antibody complexes to the nanowire surface:[31,32] low sensitivity where *d*BS extends beyond λD and high sensitivity where *d*BS is within λD. In typical buffers, the *d*BS can varied from short (*d*BS ~ 4-5 nm) to long (*d*BS ~14-15 nm) distance depending on the conformation of the binding complex target-receptor (Supplementary Table S1, Figure S3). In the immobilization scheme used here, surface conjugated antibodies are randomly oriented and separated from each other[31,35] which is expected to lead to a range of *dBS* for the proteinaceous target and therefore sufficient sensitivity under the experimental conditions used here (λD ~8 nm). Beyond these considerations, the charge density of the target protein should also be taken into consideration in determining the molecular sensitivity as discussed elsewhere.[36]

From these measurements, a LOD of ~80 fM (~3.2 pg/mL) has been calculated with three times the standard deviation of nonspecific noise in pure serum (Figure 2b). In comparison with immunometric assays (*e.g.* ELISA and EPISPOT)[27] commonly used for the detection of KRT, the SiNW FET biosensing platform provided at least two orders of magnitude improved sensitivity. The ultra-high sensitivity of the optimized SiNW FET platform is a significant step

toward the development of intraoperative sensing device able to detect reliably low concentrations of DTC in resected or biopsied biological specimens.

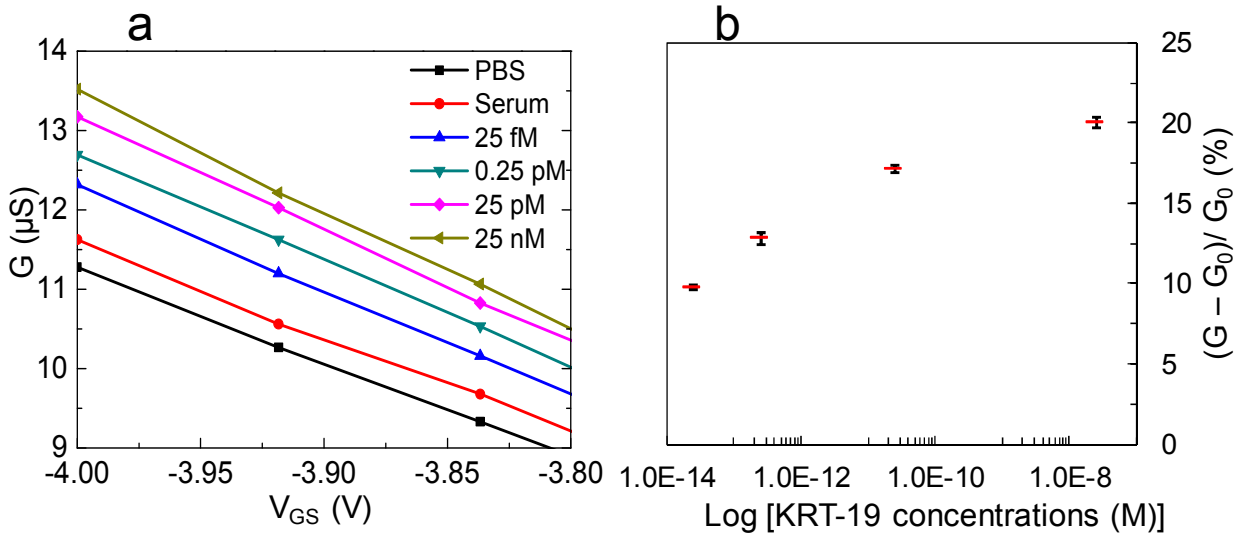

Figure 2. (a) Conductance response of a SiNW FET biosensor recorded from 0 – 25 fM – 0.25 pM – 25 pM and 25 nM of KRT-19; V_{DS} = -1.5 V. The graph shows an increase of the nanowire conductance when negatively charged KRT-19 antigens selectively bind to the immobilized antibody on the *p*-type SiNWs. (b) Percentage (%) of nanowire conductance change (error bars represent standard deviations from three different sensing channels) *vs.* logarithmic concentrations of KRT-19 biomarkers from 25 fM – 25 nM. The limit of detection was calculated to be ~80 fM.

Having demonstrated the excellent sensitivity to KRT of the SiNW FET platform, we next aimed to demonstrate its applicability to detection of small concentrations of DTC in lymph nodes. A major and often overlooked aspect of molecular sensing schemes with biological specimens is design of optimal sample preparation methodologies. This is especially significant in the context of intraoperative applications where sensitivity and reliability need to be achieved within a short time-frame. In order to facilitate the development of the molecular assay, the amount of

lymphoid cells in lymphatic tissues was first measured. To this end, a total of 13 rat LNs were homogenized to release lymphoid cells which were then enumerated as described in Figure 1c and the Supporting Note 3. Figure 3a shows a linear contour distribution of the cell number plot against LNs with different weights and average diameters. From the chart, the number of lymphoid cells in a LN can be quickly estimated based on its weight and diameter. Next the homogenization and lysing of LNs was optimized to enable rapid and reliable dissociation of lymphoid tissues and release of intracellular components. In a typical experiment, LN lysates containing approximately ~10^5 lymphoid cells/mL were prepared from frozen rat LNs and were then spiked with known concentrations of breast cancer cell MCF-7 lysate. To increase the clinical scope of the developed sensing platform, an anti-pan KRT antibody targeting KRT 4, 5, 6, 8, 10, 13, and 18 was used instead of anti-KRT-19. Anti-pan KRT antibody is the most frequently used immuno-marker for the clinical demonstration of micro-metastases or disseminated carcinoma cells in LNs.[37,38] Figure 3b presents the relative conductivity change of the SiNW FET plotted as a function of the logarithm of MCF-7 cancer cell lysate concentrations, spiked in a fixed concentration of LN lysate (calculated at ~10^5 lymphoid cells/mL). From the inset Figure 3b, it can be seen that the total conductance of the sensing channels increase when the spiked cancer cell concentration rises from 10^1 to 10^6. On the other hand, only a minor conductivity change is observed for the control channel in the same chip. These measurements show the specific nature of the cancer cell detection. From the measurement data, the detection sensitivity is calculated at ~1300 cancer cells/mL of LNs lysate (~10^5 lymphoid cells), which is equivalent to a detection sensitivity of ~1.3 cancer cells in 1 μL detection volume. The total time required for both sample preparation and subsequent measurement is 25-30 minutes. Thus, limit of detection and total measurement time are comparable to that of previously reported magnetic

resonance sensors[39] and current intraoperative PCR gold standard assays,[12,40] including OSNA.[17] Not surprisingly considering the biological complexity of the un-purified LN lysate, this sensitivity is several orders of magnitude lower than that obtained for KRT-19 in serum. In addition, this could be related to the suboptimal extraction of the poorly soluble KRT proteins from LNs tissue.

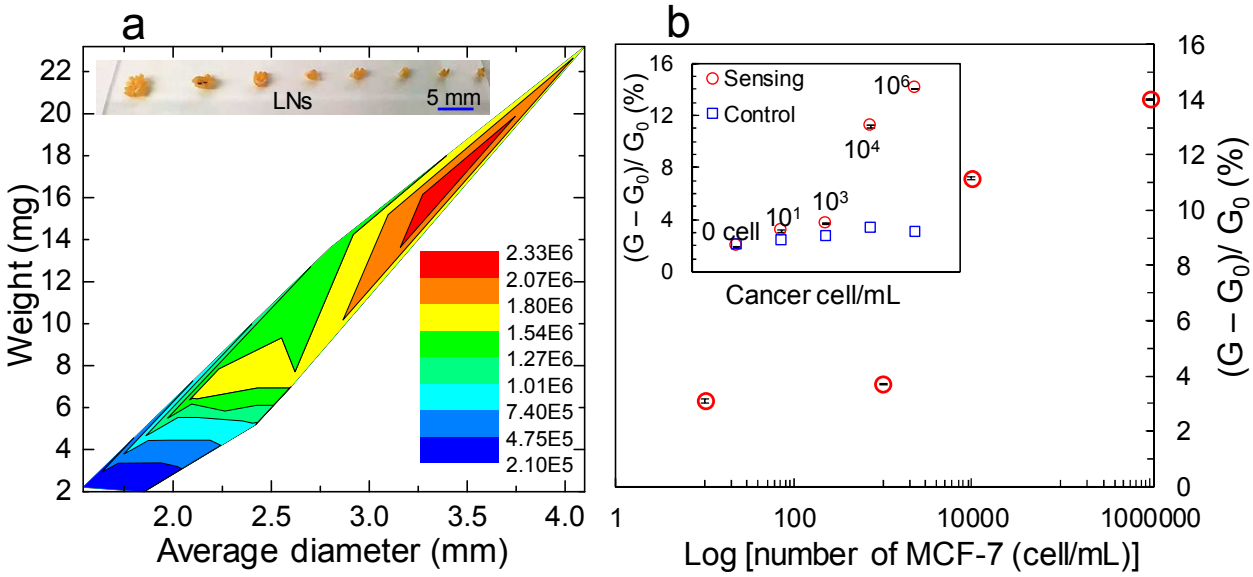

Figure 3. (a) Linear contour plot representation of cell number distribution in rat LN. Cell enumeration has been carried out in triplicate for each sample (see Supplementary Table S2). Number of sample plot (n): 13 LNs. (b) Plot of conductance responses of SiNW FET biosensor measured in the un-purified MCF-7 cancer cell lysate (10^1 - 10^6 cell/mL, in logarithmic scale) spiked in lymphoid cell lysate (10^5 cells/mL). Inset shows the detection response of sensing channels and control channels. The conductance values were calculated at the same operation point (V_{DS} = -1.25, V_{GS} = -4.5 V) for all of the SiNW channels. Error bars represent standard deviations from three different sensing channels for all the concentration experiments.

Aiming to improve the efficiency of KRT extraction and consequently the overall sensitivity of the SiNW FET bio-assay, a two-step sample preparation procedure was next developed to enrich the insoluble KRT fraction. In this protocol, LNs lysates containing various quantities of cancer cells were lysed with a lysing buffer without urea (used to solubilize KRT in the one-step assay) and centrifuged to precipitate the insoluble KRT fragments. Supernatants were then discarded and insoluble materials were re-dispersed in a KRT solubilizing buffer containing urea. SiNW FETs measurements were then conducted following the same methods described for the un-purified sample. Figure 4 shows the response of SiNW FET biosensors to different concentrations of purified lysates. A clear increase of the nanowire conductance has been observed in the plot with increasing MCF-7 concentration from 0.1, 10, 100 and 1000 cancer cells/mL of background lysate concentration. On the other hand, no significant conductance increase (<3% of the nanowires total conductance) was observed for the control channel without pan-KRT antibody functionalization, confirming the selectivity of the nanosensor (inset plot Figure 4). The limit of detection has been calculated to be ~0.01 MCF-7 cancer cells/mL or ~1 cancer cell/10^7 lymphoid cells. This result surpasses the detection sensitivity of the unpurified LN lysate measurement by several orders of magnitude and is consistent with the KRT protein detection in serum. Here, the ultra-sensitivity of the nanosensor is attributed to the efficient sample lysing and extraction of the KRT. The improved detection sensitivity emphasizes the importance of sample preparation in molecular assays. In comparison with other molecular assays (*i.e.* RT-PCR), the obtained sensitivity is at least 10 times higher than that reported for the detection of breast and colon cancer metastases in LNs (about 1 cancer cell per $10^{5\text{-}6}$ healthy lymphoid cells).[41,42] Moreover, compared with the intraoperative OSNA assay the nanowire has an increased sensitivity and would be able to detect isolated tumor cells (≤0.2 mm and <1000

tumor cells within a lymph node), which currently is the detection limit of OSNA.[17] Although the two-step sample preparation method increases the overall assay duration (approximately 55-60 min in comparison to 30 min for the one-step assay), it allows for full advantage of the exquisite sensitivity of SiNW FET biosensors. Importantly, even with the two-step enrichment protocol, the completed measurements are acquired within an hour which is comparable to current intraoperative diagnosis.[16,17]

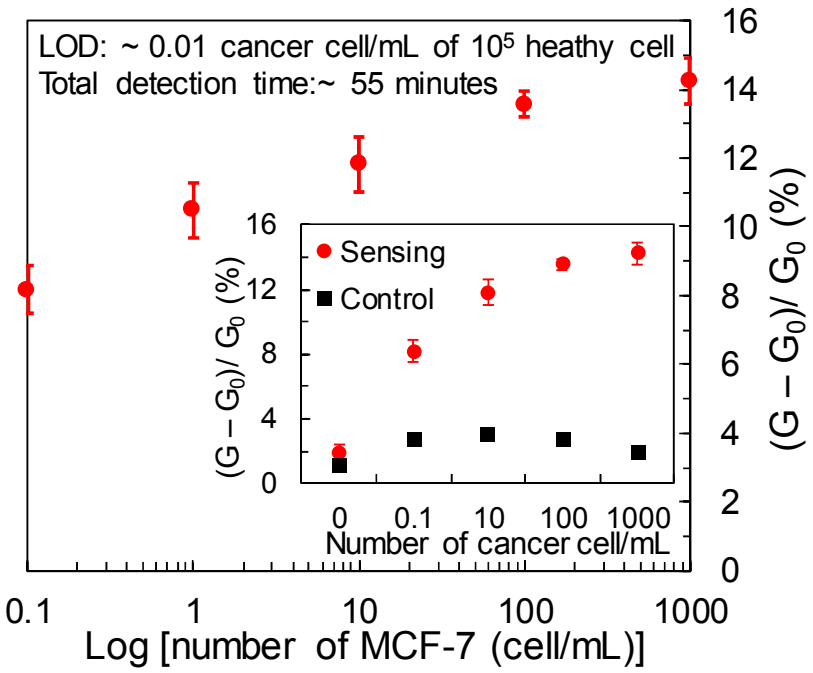

Figure 4. Response of the SiNW FET biosensor (%, $\Delta G/G0$) to different concentrations of MCF-7 cancer cells spiked in LNs (0.1 – 1000 cells/mL, in logarithmic scale). The two-step KRT enrichment protocol was used. The inset displays the specific detection of sensing channels *vs.* the control channel. The measurements are carried out at the operational point (V_{DS} = -1.5 V and V_{GS} = -4.5 V).

Building on the excellent sensitivity obtained with the LN sample, we next aimed to investigate the performance of SiNW FET in examining a patient blood specimen for the presence of

circulating tumor cells (CTCs). Detection and phenotypical analysis of CTCs in blood of patients is one of the most significant recent developments in clinical diagnostics and prognostics.[43,44] The presence of CTCs in peripheral blood has indeed been linked to early recurrence and decreased progression free survival for both metastatic and localized diseases. CTCs are, however, typically present in very small numbers in comparison to leukocytes (typically 1-10 CTC *per* 10^6 cells).[44–46] Therefore, ultra-high resolution biosensor platforms are required for reliable molecular detection of KRT markers associated with the presence of CTCs in the blood. The SiNW FET platform was utilized for detection of CTCs in colorectal cancer patient's blood. Blood samples from a colorectal patient with stage IIIB and a healthy donor were collected. The presence of CTCs in the blood sample was first confirmed using imaging flow cytometry.[47,48] Imaging flow cytometry which is a combination of flow cytometry and microscopy is advantageous for this purpose compared to microscopy alone due to its high throughput quantitative nature. Moreover, imaging flow cytometry is also advantageous compared to conventional flow cytometry as it offers the ability to visualize events and therefore, enables the exclusion of false positives and the inclusion of double positive events which would otherwise be excluded (*i.e.* a KRT + CTC and a CD45+ WBC as one event as in Figure 5a). In this technique, CTCs and white blood cells (WBCs) were selectively tagged by florescent antibodies (*e.g.* anti-KRT for CTCs and CD45 for WBCs) and later identified through the high-speed imaging system (Supporting Note 4). As shown in Figure 5, 16 CTCs (defined here using the most widely used criteria: KRT+, CD45- and DAPI+) could be detected by the imaging flow cytometer in 4 mL of patient blood. No KRT positive event was observed in the healthy blood sample control.

To carry out the SiNW FET analysis, peripheral blood mononuclear cells (PBMC) from blood samples were obtained using standard Ficoll gradient centrifugation (Supporting Note 4) and

lysed using the two-step-protocol. The conductance responses of the SiNW FETs functionalized with the anti-pan KRT was then recorded on the sensing (SS) and control (CT) channels for both samples (Figure 5b). Each measurement was conducted in at least 5 different and independent channels (n≥5). Sensing channels showed an average increase of 8.9 % of the total conductance in response to the positive sample, significantly higher than that measured on the sensing channels exposed to healthy blood sample at 2.9 %, P <0.05(Student's t-test). In addition, control channels showed less than 2% of total conductance change after exposure to both healthy and positive samples (1.9 ± 0.48 % and 1.1 ±0 .15 % respectively). The latter increases can be related to non-specific fouling of the sensor surfaces. Although further studies with a larger number of patients are required to fully validate the method, these results demonstrate the potential of the SiNW FET platform to detect clinically relevant concentrations of cancer cells in peripheral blood. Once validated clinically in a large cohort of patients, the possibility to reliably detect CTC concentrations as low as 2.5 cells/mL of blood could establish SiNW FET biosensors as an advantageous alternative to the currently used molecular approaches based on RT-PCR.

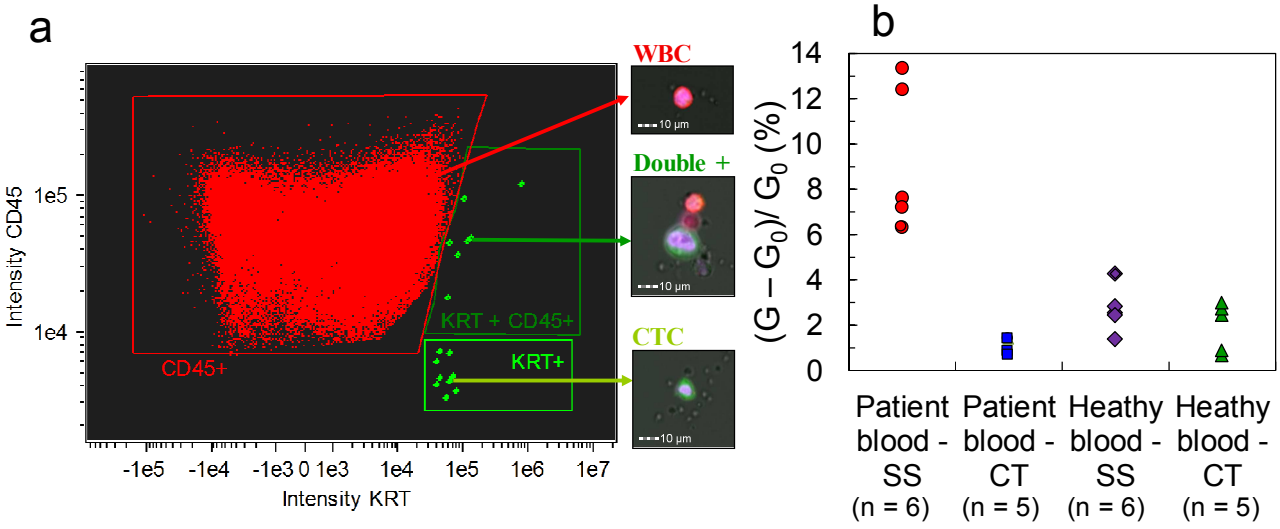

Figure 5. (a) Scatter plot of leucocyte common antigen (CD45) and KRT fluorescent markers produced from a patient's blood sample using imaging flow cytometry. Inset: typical positive

white blood cell (WBCs), double positive WBC and CTC, and CTC. (b) Validation of the SiNW FET platform for the detection of CTCs in peripheral blood. SS and CT: sensing and control channels, respectively; *n* is the number of measured channels.

CONCLUSIONS. In summary, the feasibility of an intraoperative sensing method based on a SiNW FET platform was demonstrated for ultrasensitive detection of DTC in lymph nodes as well as CTCs in peripheral blood. A holistic approach was used to optimize the fabrication and integration of the SiNW FET sensing platform as well as to optimize the sample preparation methodology. Most significantly, as small as 0.01 tumor cells per milliliter of lymph node lysate could be detected within an hour which would translate into the possibility to detect single tumor cells in a whole lymph node, surpassing the current and emerging gold standards in both sensitivity of detection and speed. While detection of protein or RNA KRTs as markers of the presence of tumor cells within biological samples is the current gold standard in immunohistochemistry and molecular systems such as OSNA, solid-state sensing platform such as the one proposed here could be readily expanded to panels of prognostic markers. Through integration of the SiNW FETs with a dedicated microfluidic platform, specific multiplexed detection could be developed, for instance for determining specific KRT expression patterns (*e.g.* KRT-16 up-regulation, associated to poor prognostic[49]) or the expression of membrane markers of relevance to a specific disease. Such developments have a strong potential to pave the way to the implementation of nanoscale FET technology in intraoperative multiplex clinical diagnostics.

METHODS

Fabrication and On-chip Packaging of SiNW FETs. The wafer-scale fabrication process of the multichannel SiNW FET arrays is modified from our previous report.[23,24] At first, a thin (44 ± 2 nm) homogenous silicon dioxide (SiO_2) layer was dry-oxidized on top of *p*-type SOI wafers (SOITEC; B: 10^{15} cm^{-3}; BOX: 145 nm; Si device layer: 70 nm). Aluminium nanostructures were then patterned on top of the SiO_2 by a lift-off process with e-beam patterning and metal evaporation on PMMA photoresist. A subsequent reactive ion-etching was performed to transfer the Al patterns to the SiO_2 beneath. After removing the entire Al pattern, the wafers were subjected in TMAH wet-etching (25wt %; 80^oC with agitation, 2-4 minutes) to define the nanowires' width. The wafers were then dry-oxidized again to form ~ 8-10 nm of SiO_2 to serve as the gate isolator layer. Source and drain contacts of the nanowire were then selectively ion-implanted (B; 10^{15} cm^{-2}) followed by an annealing step with a stack of patterned Al/Cr/Ag for metal feedlines. Finally, a thin passivation layer of SiO_2/Si_3N_4 (~ 1 μm thickness) was deposited using PECVD and patterned with reactive ion etching on the wafers to electrically isolate the feed lines during the wet-measurement. The wafers were finally diced in small (18 x 8 mm) ready-to-test chips and packaged in a dual in-line package (DIP-24) ceramic socket. Aiming for everyday diagnostic test, a customized headstage with two zero-insertion-force (ZIF) sockets has been built and integrated with a developed multichannel amplifier. By connecting the SiNWs device *via* the DIP housing inserted in the ZIF sockets, multiple measurements could be performed easily without mechanically degrading the metal electrodes due to the frequent contact with the needle of a probe station.

Surface Functionalization. Based on our previously developed protocol,[50] the surface functionalization of SiNWs has been performed by employing 3-aminopropyl triethoxysilane

(APTES) vapor-phase silanization followed by reaction with glutaraldehyde and finally with a monoclonal antibody against cytokeratin. Only the sensing channels were functionalized with the antibody and a control channel was kept un-functionalized to serve as a reference for non-specific adsorption events. A blocking solution composed of 1% BSA and 0.1% Tween 20 was finally used in all channels to minimize non-specific adsorption.

SiNW FETs measurement. Typically, ~40 μL of sample solution was incubated for 10 minutes, followed by 3-5 minutes of intensive washing with 1X PBS (pH 7.4). Electrical characterizations were performed simultaneously in the sensing and control channels with fresh 0.01X PBS (pH 7.4, room temperature) though the whole biological measurements in this work. The sensitivity of the device was calculated from the relative change of the nanowires conductivity ($\Delta G/G0$, %) in response to the presence of the antigen at the device maximum transconductance (*g*m). The maximum *g*m was determined from the transfer characteristic curves at the beginning of the experiment and was kept constant during the concentration measurement. $G0$ is the initial conductance of the nanowires measured in the fresh 0.01X PBS.

Lymph node lysate preparation protocols

Un-purified sample preparations: A lysing buffer containing 0.1M Tris-HCl, 1M NaCl, 0.1M EDTA (pH 8.0), 8 M Urea, 1% Sodium Deoxycholate, 1% Triton-X100, 10% Glycerol, 5% SDS and 2mM DTT has been prepared and used fresh to separately lyse and solubilize the total protein from lymph node and MCF-7 cancer cell line samples. All reagents and solvents (reagent grade) were from Sigma-Aldrich (US) and used as received. For extraction and solubilisation of total protein in one-step, the number of lymphoid cells was first estimated based on the average diameter and weight of the LNs. To assist the cell lysing, a quick homogenization (3 minutes)

has been performed on ice in the prepared buffer. Next, the homogenizer was washed and the cell solution was sonicated in an ultrasonic bath for 10 minutes. In the meantime, MCF-7 cells were harvested and lysed in the developed lysing buffer inside an ultrasonic bath for 10 minutes. The prepared cell lysates were freshly used.

Purified sample preparations: In this protocol, LNs were first homogenized with a dounce homogenizer. Lymphoid cells were then pre-cleaned and harvested with centrifugation. Both lymphoid and MCF-7 cells were then subjected to the cell lysing step using ultrasonic bath (10 minutes) in a cell lysis buffer (Tris-HCl 0.1 M, NaCl 1 M, EDTA 0.1 M, Urea 1 M, Sodium deoxycholate, Triton X-100, Glycerol, SDS 10% , milliQ water; pH 7.4). Next, the cell lysate solutions were centrifuged (14000 rcf, 15 minutes, 4 ^{o}C) and supernatants were discarded. The insoluble pellets were finally dissolved in the protein extraction buffer (Tris-HCl 0.03M, Urea 9.5 M, DTT 0.002M, EDTA 0.002M; pH 8.0), followed by a short ultra-sonication for 3 minutes. For confirming the lysis process, all of the lysed samples were checked under microscope for cell debris and later with UV-vis for total protein extraction. The cell harvesting, lysing and protein extraction were all performed on ice (4^{o}C) to prevent the protein denaturation.

Supporting Information. Detail of the electrical characterization; calculation of Debye screening length and *dBS* length; lymph node homogenization and enumeration; cancer patient blood preparation protocol and detail of imaging flow cytometry. This information is available free of charge *via* the Internet at http://pubs.acs.org.

Author Contributions. All authors have contributed and given approval to the final version of the manuscript.

Author Information

Corresponding Author:

Benjamin Thierry. Email: Benjamin.thierry@unisa.edu.au

Andreas Offenhäusser. Email: a.offenhaeusser@fz-juelich.de

Acknowledgements. This work is supported by a NHMRC project grant as well as by a grant from the joint initiative of the Australian Technology Network of Universities (ATN) and the German Academic Exchange Service (DAAD). The authors also would like to thank Dr. Dirk Mayer and technicians in the Forschungszentrum Jülich; ANFF-SA node for their help and support; Prof. Rachel Gibson, Tim Price, Jenny Hardingham and Joseph Wrin for providing the biological specimens.

References

1. Raia-Barjat, T.; Trombert, B.; Khaddage, A.; Douchet, C.; Seffert, P.; Peoc'h, M.; Falk, A. T.; Magné, N.; Chauleur, C. OSNA (one-Step Nucleic Acid Amplification) Sentinel Lymph Node Intraoperative Molecular Analysis in Breast Cancer: A Cost-Benefit Analysis. *Med. Oncol.* **2014**, *31*, 1–8.
2. Guillén-Paredes, M. P.; Carrasco-González, L.; Cháves-Benito, A.; Campillo-Soto, Á.; Carrillo, A.; Aguayo-Albasini, J. L. One-Step Nucleic Acid Amplification (OSNA) Assay for Sentinel Lymph Node Metastases as an Alternative to Conventional Postoperative Histology in Breast Cancer: A Cost-Benefit Analysis. *Cir. Esp. Engl. Ed.* **2011**, *89*, 456–462.
3 Langer, I.; Guller, U.; Berclaz, G.; Koechli, O. R.; Schaer, G.; Fehr, M. K.; Hess, T.; Oertli, D.; Bronz, L.; Schnarwyler, B. Morbidity of Sentinel Lymph Node Biopsy (SLN) Alone versus SLN and Completion Axillary Lymph Node Dissection after Breast Cancer Surgery: A Prospective Swiss Multicenter Study on 659 Patients. *Ann. Surg.* **2007**, *245*, 452.
4. Schrenk, P.; Rieger, R.; Shamiyeh, A.; Wayand, W. Morbidity Following Sentinel Lymph Node Biopsy versus Axillary Lymph Node Dissection for Patients with Breast Carcinoma. *Cancer* **2000**, *88*, 608–614.
5. Jenkins, V.; Harder, H.; Babar, M.; Merry, S.; Newbury, S.; Kissin, M.; Zammit, C. A Pilot Study to Examine the Experiences and Attitudes of Women with Breast Cancer towards One versus Two-Step Axillary Surgery. *The Breast* **2012**, *21*, 72–76.
6. Leong, S. P.; Tseng, W. W. Micrometastatic Cancer Cells in Lymph Nodes, Bone Marrow, and Blood: Clinical Significance and Biologic Implications. *CA. Cancer J. Clin.* **2014**, *64*, 195–206.

7. Pantel, K.; Cote, R. J.; Fodstad, Ø. Detection and Clinical Importance of Micrometastatic Disease. *J. Natl. Cancer Inst.* **1999**, *91*, 1113–1124.
8. Cserni, G. A Model for Determining the Optimum Histology of Sentinel Lymph Nodes in Breast Cancer. *J. Clin. Pathol.* **2004**, *57*, 467–471.
9. Murali, R.; DeSilva, C.; McCarthy, S. W.; Thompson, J. F.; Scolyer, R. A. Sentinel Lymph Nodes Containing Very Small (< 0.1 Mm) Deposits of Metastatic Melanoma Cannot Be Safely Regarded as Tumor-Negative. *Ann. Surg. Oncol.* **2012**, *19*, 1089–1099.
10. Yu, Y.-H.; Wei, W.; Liu, J.-L. Diagnostic Value of Fine-Needle Aspiration Biopsy for Breast Mass: A Systematic Review and Meta-Analysis. *BMC Cancer* **2012**, *12*, 41.
11. Ferris, R. L.; Xi, L.; Seethala, R. R.; Chan, J.; Desai, S.; Hoch, B.; Gooding, W.; Godfrey, T. E. Intraoperative qRT-PCR for Detection of Lymph Node Metastasis in Head and Neck Cancer. *Clin. Cancer Res.* **2011**, *17*, 1858–1866.
12. Castellano, I.; Macrì, L.; Deambrogio, C.; Balmativola, D.; Bussone, R.; Ala, A.; Coluccia, C.; Sapino, A. Reliability of Whole Sentinel Lymph Node Analysis by One-Step Nucleic Acid Amplification for Intraoperative Diagnosis of Breast Cancer Metastases. *Ann. Surg.* **2012**, *255*, 334–342.
13. Viale, G.; Dell'Orto, P.; Biasi, M. O.; Stufano, V.; Lima, L. N. D. B.; Paganelli, G.; Maisonneuve, P.; Vargo, J. M.; Green, G.; Cao, W. Comparative Evaluation of an Extensive Histopathologic Examination and a Real-Time Reverse-Transcription-Polymerase Chain Reaction Assay for Mammaglobin and Cytokeratin 19 on Axillary Sentinel Lymph Nodes of Breast Carcinoma Patients. *Ann. Surg.* **2008**, *247*, 136–142.
14. Masai, K.; Nakagawa, K.; Yoshida, A.; Sakurai, H.; Watanabe, S.; Asamura, H.; Tsuta, K. Cytokeratin 19 Expression in Primary Thoracic Tumors and Lymph Node Metastases. *Lung Cancer* **2014**.
15. Mikhitarian, K.; Gillanders, W. E.; Almeida, J. S.; Martin, R. H.; Varela, J. C.; Metcalf, J. S.; Cole, D. J.; Mitas, M. An Innovative Microarray Strategy Identities Informative Molecular Markers for the Detection of Micrometastatic Breast Cancer. *Clin. Cancer Res.* **2005**, *11*, 3697–3704.
16. Klingler, S.; Marchal, F.; Rauch, P.; Kenouchi, O.; Chrétien, A.-S.; Genin, P.; Leroux, A.; Merlin, J.-L. Using One-Step Nucleic Acid Amplification (OSNA) for Intraoperative Detection of Lymph Node Metastasis in Breast Cancer Patients Avoids Second Surgery and Accelerates Initiation of Adjuvant Therapy. *Ann. Oncol.* **2013**, mdt160.
17. Visser, M.; Jiwa, M.; Horstman, A.; Brink, A. A.; Pol, R. P.; van Diest, P.; Snijders, P. J.; Meijer, C. J. Intra-operative Rapid Diagnostic Method Based on CK19 mRNA Expression for the Detection of Lymph Node Metastases in Breast Cancer. *Int. J. Cancer* **2008**, *122*, 2562–2567.
18. Patolsky, F.; Zheng, G.; Lieber, C. M. Fabrication of Silicon Nanowire Devices for Ultrasensitive, Label-Free, Real-Time Detection of Biological and Chemical Species. *Nat Protoc.* **2006**, *1*, 1711–1724.
19. Gao, A.; Lu, N.; Dai, P.; Li, T.; Pei, H.; Gao, X.; Gong, Y.; Wang, Y.; Fan, C. Silicon-Nanowire-Based CMOS-Compatible Field-Effect Transistor Nanosensors for Ultrasensitive Electrical Detection of Nucleic Acids. *Nano Lett.* **2011**, *11*, 3974–3978.
20. Zheng, G.; Patolsky, F.; Cui, Y.; Wang, W. U.; Lieber, C. M. Multiplexed Electrical Detection of Cancer Markers with Nanowire Sensor Arrays. *Nat Biotech* **2005**, *23*, 1294–1301.

21. Makowski, M. S.; Ivanisevic, A. Molecular Analysis of Blood with Micro-/Nanoscale Field-Effect-Transistor Biosensors. *Small* **2011**, *7*, 1863–1875.
22. Stern, E.; Klemic, J. F.; Routenberg, D. A.; Wyrembak, P. N.; Turner-Evans, D. B.; Hamilton, A. D.; LaVan, D. A.; Fahmy, T. M.; Reed, M. A. Label-Free Immunodetection with CMOS-Compatible Semiconducting Nanowires. *Nature* **2007**, *445*, 519–522.
23. Tran, D. P.; Wolfrum, B.; Stockmann, R.; Pai, J.-H.; Pourhassan-Moghaddam, M.; Offenhäusser, A.; Thierry, B. Complementary Metal Oxide Semiconductor Compatible Silicon Nanowires-on-a-Chip: Fabrication and Preclinical Validation for the Detection of a Cancer Prognostic Protein Marker in Serum. *Anal. Chem.* **2015**, *87*, 1662–1668.
24. Tran, D. P.; Wolfrum, B.; Stockmann, R.; Offenhausser, A.; Thierry, B. Fabrication of Locally Thinned down Silicon Nanowires. *J. Mater. Chem. C* **2014**, *2*, 5229–5234.
25. Eschermann, J. F.; Stockmann, R.; Hueske, M.; Vu, X. T.; Ingebrandt, S.; Offenhausser, A. Action Potentials of HL-1 Cells Recorded with Silicon Nanowire Transistors. *Appl. Phys. Lett.* **2009**, *95*, 083703–3.
26. Stathopoulou, A.; Vlachonikolis, I.; Mavroudis, D.; Perraki, M.; Kouroussis, C.; Apostolaki, S.; Malamos, N.; Kakolyris, S.; Kotsakis, A.; Xenidis, N. Molecular Detection of Cytokeratin-19–positive Cells in the Peripheral Blood of Patients with Operable Breast Cancer: Evaluation of Their Prognostic Significance. *J. Clin. Oncol.* **2002**, *20*, 3404–3412.
27. Alix-Panabières, C.; Vendrell, J.-P.; Slijper, M.; Pellé, O.; Barbotte, E.; Mercier, G.; Jacot, W.; Fabbro, M.; Pantel, K. Full-Length Cytokeratin-19 Is Released by Human Tumor Cells: A Potential Role in Metastatic Progression of Breast Cancer. *Breast Cancer Res* **2009**, *11*, R39.
28. Saloustros, E.; Mavroudis, D. Cytokeratin 19-Positive Circulating Tumor Cells in Early Breast Cancer Prognosis. *Future Oncol.* **2010**, *6*, 209–219.
29. Chen, Y.; Zou, T. N.; Wu, Z. P.; Zhou, Y. C.; Gu, Y. L.; Liu, X.; Jin, C. G.; Wang, X. C. Detection of Cytokeratin 19, Human Mammaglobin, and Carcinoembryonic Antigen-Positive Circulating Tumor Cells by Three-Marker Reverse Transcription-PCR Assay and Its Relation to Clinical Outcome in Early Breast Cancer. *Int. J. Biol. Markers* **2009**, *25*, 59–68.
30. Stern, E.; Wagner, R.; Sigworth, F. J.; Breaker, R.; Fahmy, T. M.; Reed, M. A. Importance of the Debye Screening Length on Nanowire Field Effect Transistor Sensors. *Nano Lett.* **2007**, *7*, 3405–3409.
31. Elnathan, R.; Kwiat, M.; Pevzner, A.; Engel, Y.; Burstein, L.; Khatchtourints, A.; Lichtenstein, A.; Kantaev, R.; Patolsky, F. Biorecognition Layer Engineering: Overcoming Screening Limitations of Nanowire-Based FET Devices. *Nano Lett.* **2012**, *12*, 5245–5254.
32. Zhang, G.-J.; Zhang, G.; Chua, J. H.; Chee, R.-E.; Wong, E. H.; Agarwal, A.; Buddharaju, K. D.; Singh, N.; Gao, Z.; Balasubramanian, N. DNA Sensing by Silicon Nanowire: Charge Layer Distance Dependence. *Nano Lett.* **2008**, *8*, 1066–1070.
33. Stern, E.; Vacic, A.; Rajan, N. K.; Criscione, J. M.; Park, J.; Ilic, B. R.; Mooney, D. J.; Reed, M. A.; Fahmy, T. M. Label-Free Biomarker Detection from Whole Blood. *Nat Nano* **2010**, *5*, 138–142.
34. Chan, R.; Rossitto, P. V.; Edwards, B. F.; Cardiff, R. D. Presence of Proteolytically Processed Keratins in the Culture Medium of MCF-7 Cells. *Cancer Res.* **1986**, *46*, 6353–6359.
35. Jung, Y.; Jeong, J. Y.; Chung, B. H. Recent Advances in Immobilization Methods of Antibodies on Solid Supports. *Analyst* **2008**, *133*, 697–701.

36. Goda, T.; Miyahara, Y. Interpretation of Protein Adsorption through Its Intrinsic Electric Charges: A Comparative Study Using a Field-Effect Transistor, Surface Plasmon Resonance, and Quartz Crystal Microbalance. *Langmuir* **2012**, *28*, 14730–14738.
37. Yang, Y.; Li, J.; Mao, S.; Zhu, H. Comparison of Immunohistology Using Pan-CK and EMA in the Diagnosis of Lymph Node Metastasis of Gastric Cancer, Particularly Micrometastasis and Isolated Tumor Cells. *Oncol. Lett.* **2013**, *5*, 768–772.
38. Xu, W.; Cao, L.; Chen, L.; Li, J.; Zhang, X.-F.; Qian, H.-H.; Kang, X.-Y.; Zhang, Y.; Liao, J.; Shi, L.-H.; *et al.* Isolation of Circulating Tumor Cells in Patients with Hepatocellular Carcinoma Using a Novel Cell Separation Strategy. *Clin. Cancer Res.* **2011**, *17*, 3783–3793.
39. Lee, H.; Yoon, T.-J.; Figueiredo, J.-L.; Swirski, F. K.; Weissleder, R. Rapid Detection and Profiling of Cancer Cells in Fine-Needle Aspirates. *Proc. Natl. Acad. Sci.* **2009**, *106*, 12459–12464.
40. Heilmann, T.; Mathiak, M.; Hofmann, J.; Mundhenke, C.; van Mackelenbergh, M.; Alkatout, I.; Wenners, A.; Eckmann-Scholz, C.; Schem, C. Intra-Operative Use of One-Step Nucleic Acid Amplification (OSNA) for Detection of the Tumor Load of Sentinel Lymph Nodes in Breast Cancer Patients. *J. Cancer Res. Clin. Oncol.* **2013**, *139*, 1649–1655.
41. Noguchi, S.; Aihara, T.; Motomura, K.; Inaji, H.; Imaoka, S.; Koyama, H. Detection of Breast Cancer Micrometastases in Axillary Lymph Nodes by Means of Reverse Transcriptase-Polymerase Chain Reaction. Comparison between MUC1 mRNA and Keratin 19 mRNA Amplification. *Am. J. Pathol.* **1996**, *148*, 649.
42. Ichikawa, Y.; Ishikawa, T.; Momiyama, N.; Yamaguchi, S.; Masui, H.; Hasegawa, S.; Chishima, T.; Takimoto, A.; Kitamura, H.; Akitaya, T. Detection of Regional Lymph Node Metastases in Colon Cancer by Using RT-PCR for Matrix Metalloproteinase 7, Matrilysin. *Clin. Exp. Metastasis* **1998**, *16*, 3–8.
43. Becker, T. M.; Caixeiro, N. J.; Lim, S. H.; Tognela, A.; Kienzle, N.; Scott, K. F.; Spring, K. J.; de Souza, P. New Frontiers in Circulating Tumor Cell Analysis: A Reference Guide for Biomolecular Profiling toward Translational Clinical Use. *Int. J. Cancer* **2014**, *134*, 2523–2533.
44. Krebs, M. G.; Metcalf, R. L.; Carter, L.; Brady, G.; Blackhall, F. H.; Dive, C. Molecular Analysis of Circulating Tumour Cells[mdash]biology and Biomarkers. *Nat Rev Clin Oncol* **2014**, *11*, 129–144.
45. Miller, M. C.; Doyle, G. V.; Terstappen, L. W. Significance of Circulating Tumor Cells Detected by the CellSearch System in Patients with Metastatic Breast Colorectal and Prostate Cancer. *J. Oncol.* **2009**, *2010*.
46. Zhe, X.; Cher, M. L.; Bonfil, R. D. Circulating Tumor Cells: Finding the Needle in the Haystack. *Am. J. Cancer Res.* **2011**, *1*, 740.
47. Reyes, E. E.; VanderWeele, D. J.; Isikbay, M.; Duggan, R.; Campanile, A.; Stadler, W. M.; Vander Griend, D. J.; Szmulewitz, R. Z. Quantitative Characterization of Androgen Receptor Protein Expression and Cellular Localization in Circulating Tumor Cells from Patients with Metastatic Castration-Resistant Prostate Cancer. *J. Transl. Med.* **2014**, *12*, 313.
48. López-Riquelme, N.; Minguela, A.; Villar-Permuy, F.; Ciprian, D.; Castillejo, A.; Álvarez-López, M.-R.; Soto, J.-L. Imaging Cytometry for Counting Circulating Tumor

Cells: Comparative Analysis of the CellSearch vs ImageStream Systems. *Apmis* **2013**, *121*, 1139–1143.

49. Joosse, S. A.; Hannemann, J.; Spötter, J.; Bauche, A.; Andreas, A.; Müller, V.; Pantel, K. Changes in Keratin Expression during Metastatic Progression of Breast Cancer: Impact on the Detection of Circulating Tumor Cells. *Clin. Cancer Res.* **2012**, *18*, 993–1003.
50. Han, Y.; Mayer, D.; Offenhäusser, A.; Ingebrandt, S. Surface Activation of Thin Silicon Oxides by Wet Cleaning and Silanization. *Thin Solid Films* **2006**, *510*, 175–180.

For Table of Contents only